Somatic retrotransposition in human cancer revealed by whole-genome and exome sequencing

Elena Helman, Michael L. Lawrence, Chip Stewart, et al.

Genome Res. published online May 13, 2014
Access the most recent version at doi:10.1101/gr.163659.113

Somatic retrotransposition in human cancer revealed by whole-genome and exome sequencing

Elena Helman[1,2], Michael S. Lawrence[2], Chip Stewart[2], Carrie Sougnez[2], Gad Getz[2,3], Matthew Meyerson[1,2,4,5]*

[1]Harvard-MIT Division of Health Sciences & Technology, Cambridge, MA, 02139.

[2]Broad Institute of MIT and Harvard, Cambridge, MA, 02142.

[3]Massachusetts General Hospital, Boston, MA, 02114.

[4]Center for Cancer Genome Discovery and Department of Medical Oncology, Dana-Farber Cancer Institute, Boston, MA, 02215.

[5]Department of Pathology, Brigham & Women's Hospital and Harvard Medical School, Boston, Massachusetts, 02115.

*To whom correspondence should be addressed. Email: matthew_meyerson@dfci.harvard.edu

Running title: Somatic retrotransposition in cancer

Abstract:

Retrotransposons constitute a major source of genetic variation, and somatic retrotransposon insertions have been reported in cancer. Here, we applied TranspoSeq, a computational framework that identifies retrotransposon insertions from sequencing data, to whole-genomes from 200 tumor/normal pairs across 11 tumor types as part of The Cancer Genome Atlas (TCGA) Pan-Cancer Project. In addition to novel germline polymorphisms, we find 810 somatic retrotransposon insertions primarily in lung squamous, head and neck, colorectal and endometrial carcinomas. Many somatic retrotransposon insertions occur in known cancer genes. We find that high somatic retrotransposition rates in tumors are associated with high rates of genomic rearrangement and somatic mutation. Finally, we developed TranspoSeq-Exome to interrogate an additional 767 tumor samples with hybrid-capture exome data and discover 35 novel somatic retrotransposon insertions into exonic regions, including an insertion into an exon of the *PTEN* tumor suppressor gene. The results of this large-scale, comprehensive analysis of retrotransposon movement across tumor types suggest that somatic retrotransposon insertions may represent an important class of structural variation in cancer.

Keywords: Retrotransposons, Lung squamous cell carcinoma, Head and neck squamous cell carcinoma, Whole-genome sequencing, Whole-exome sequencing, Genomic rearrangements

Introduction:

Retrotransposons are genomic elements that mobilize via an RNA intermediate in a copy-and-paste mechanism across the genome. Regarded as "drivers of genome evolution", retrotransposons comprise nearly half of the human genome and are important vehicles of genomic diversity {Lander:2001hk, Kazazian:2004bf}. Although the majority of these elements are inactive ancient insertions, a small proportion retains their retrotransposition capacity (Brouha et al. 2003; Beck et al. 2010). The three most active retrotransposon families known are the Long INterspersed Element (LINE-1 or L1), *Alu*, and SVA (SINE/VNTR/*Alu*) families (Xing et al. 2009; Kimberland et al. 1999; Moran et al. 1996), specifically the L1HS, *Alu*Ya5 and *Alu*Yb8 subfamilies in humans (Burns and Boeke 2012). These are thought to retrotranspose via a target-primed reverse transcription (TPRT) mechanism (Lander et al. 2001; Ostertag and Kazazian 2001; Kazazian 2004; Luan et al. 1993; Jurka 1997; Luan and Eickbush 1995; Cost et al. 2002), wherein the L1-endonuclease creates two nicks in the genomic DNA followed by insertion of a new copy of the element into the lesion, resulting in short duplicated sequences surrounding the insertion.

Retrotransposon insertions are coming to light as a major source of genetic variation (Brouha et al. 2003; Ewing and Kazazian 2011; Beck et al. 2010; Stewart et al. 2011). It is estimated that 1 of every 20 live human births exhibits a *de novo* retrotransposon insertion (Xing et al. 2009; Cordaux and Batzer 2009; Kimberland et al. 1999; Moran et al. 1996). A pair of individuals of European origin are believed to differ by approximately 500-800 retrotransposon insertion polymorphisms (Burns and Boeke 2012; Stewart et al. 2011). Depending on where they land in the genome, retrotransposon insertions can affect protein function, alter gene expression, and catalyze genomic instability. Over 90 germline retrotransposon insertions have been

implicated in disease (Hancks and Kazazian 2012). Specific instances of putative somatic retrotransposon insertions have previously been identified in cancer, including insertions of L1 elements in an exon of the *APC* tumor suppressor gene in a case of colorectal cancer (Miki et al. 1992) and within the *MYC* gene in a breast carcinoma specimen (Morse et al. 1988), although only the APC event has been verified as a *bona-fide* L1 insertion. Experimental approaches have since identified nine somatic L1 insertions in six primary non-small cell lung tumors (Iskow et al. 2010), numerous L1 insertions in 16 colorectal tumors (Solyom et al. 2012) and a somatic insertion in *ST18* in hepatocellular carcinoma (Shukla et al. 2013).

The advent of next-generation sequencing studies of cancer (Meyerson et al. 2010; Stratton et al. 2009) now provides the opportunity to comprehensively investigate the extent of somatic retrotransposon insertions. A recent study identified almost two hundred putative somatic retrotransposon insertions from 43 tumor genomes (Lee et al. 2012). Here, we analyze 200 tumor/normal pairs across 11 cancer types using TranspoSeq, a tool we developed to localize retrotransposon insertions from paired-end sequencing data. We find a total of 810 somatic retrotransposon insertions, with 324 in 19 lung squamous cell carcinomas and 206 in 28 head and neck squamous cell carcinomas, while other tumor types appear comparatively quiet. Some of these insertions mobilize to genic regions, including exons, and genes previously implicated in cancer progression. We expand our search to exome data using a modified tool and find additional somatic insertions into exons in endometrial carcinoma.

Results:

Whole-genome sequencing reveals numerous non-reference retrotransposon insertions

To identify non-reference somatic retrotransposon insertions computationally from whole-genome sequencing data, we developed TranspoSeq (Helman and Meyerson 2011a; http://cancergenome.nih.gov/newsevents/multimedialibrary/videos/retroseqhelman). Briefly, TranspoSeq locates clusters of unique sequencing reads whose pair-mates align to a database of consensus retrotransposon sequences and predict a genomic fragment length that is non-concordant with the fragment length distribution of the sample (Supplemental Fig. 1). TranspoSeq classifies putative novel retrotransposon insertion sites as germline, present in both tumor and normal samples but not in the reference, or as somatic, present only in the tumor. We assessed TranspoSeq's performance using simulated data, determining a sensitivity of 99% with no false positive calls and a drop in sensitivity at inserted element lengths of <100bp (Supplemental Fig. 2). We also compared TranspoSeq's performance to other methods on the same individual and find high concordance (Keane et al. 2013; Lee et al. 2012) (Supplemental Material). Finally, we ran TranspoSeq on swapped tumor and normal samples and found no spurious retrotransposon insertions unique to the matched normal tissue (Supplemental Material).

To determine the extent of somatic retrotransposon activity across cancer, we applied TranspoSeq to whole-genome sequencing data from 200 tumor and matched normal samples collected and sequenced through The Cancer Genome Atlas across 11 tumor types: lung adenocarcinoma (LUAD), lung squamous cell carcinoma (LUSC), ovarian carcinoma (OV), rectal adenocarcinoma (READ), colon adenocarcinoma (COAD), kidney clear cell carcinoma (KIRC), uterine corpus endometrioid carcinoma (UCEC), head and neck squamous cell

carcinoma (HNSC), breast carcinoma (BRCA), acute myeloid leukemia (LAML), and glioblastoma multiforme (GBM). We identified 7,724 unique, non-reference germline insertion sites seen in both tumor and matched normal samples (Supplemental Table 2). Of these, 65% are known retrotransposon insertion polymorphisms annotated in previous studies (Lee et al. 2012; Beck et al. 2010; Huang et al. 2010; Hormozdiari et al. 2010; Iskow et al. 2010; Witherspoon et al. 2010; Stewart et al. 2011; Ewing and Kazazian 2010; 2011; Xing et al. 2009). Many of the novel germline retrotransposon insertions identified here represent previously unannotated common polymorphisms, present in as many as 114 individuals (Supplemental Fig. 3D).

We attempted experimental validation on a set of 47 putative somatic retrotransposon insertions, across 21 individuals and 4 tumor types, including 5 somatic insertions identified from exome data, as well as 4 predicted germline transpositions. Validation was carried out via site-specific PCR designed to span the 5' and 3' junctions of candidate insertions for tumor and matched normal samples, followed by Illumina sequencing. We found 39/47 (83%) of predicted somatic insertions have experimental evidence for a transposition event by amplification of either 5' or 3' junctions in the tumor, but no junctional amplification from the matched normal sample. Moreover, 32 of 47 (68%) predicted somatic insertions had evidence for amplification of both 5' and 3' junctions in the tumor sample and no evidence in the matched normal. Finally, 2/47 putative somatic retrotranspositions had some evidence of the insertion in the matched normal, and 6/47 failed to produce any amplicons in either tumor or matched normal (Supplemental Table 1).

Somatic retrotransposon insertion rates vary across tumor types

We detected a total of 810 putative retrotransposon insertions occurring in cancer DNA but not in matched normal DNA from the same patient. These candidate somatic retrotransposition events exhibit the hallmarks of target-primed reverse transcription, such as target site duplications (TSDs) ~15bp in length (Fig. 1A), and a canonical L1-endonuclease motif (Lander et al. 2001; Feng et al. 1996; Kazazian 2004; Morrish et al. 2002) at the site of insertion (Fig. 1B). There is an additional class of somatic events lacking a TSD, however, suggesting a possible alternative mechanism for somatic insertion (Supplemental Fig. 5). Consistent with previous reports (Brouha et al. 2003; Lee et al. 2012; Beck et al. 2010; Solyom et al. 2012; Iskow et al. 2010), we find that somatic insertions consist primarily (97%) of L1HS elements, specifically L1HS elements that are severely 5' truncated, differing significantly from germline insertions (Fig. 1C-D). In addition, we find several full-length L1HS somatic insertions, as well as one putative somatic insertion of an SVA element (Supplemental Table 3). It should be noted that, given the 83% validation rate of TranspoSeq, it is likely that roughly 670 of the 810 putative somatic insertions are real events while the remaining may be false positives, due to sequencing artifact or presence in normal tissue.

Somatic retrotransposon insertions display a tumor-specific pattern. While GBM, LAML, BRCA, KIRC, OV, and LUAD samples exhibit little or no detected somatic retrotransposition, LUSC, COAD/READ, HNSC, and UCEC show active mobilization of retrotransposons (Fig. 1E, Supplemental Fig. 4 and Supplemental Table 3). These findings are in accordance with other studies where L1 insertions were seen in epithelial cancers but not in glioblastomas or hematopoietic cancers (Xing et al. 2009; Iskow et al. 2010; Kimberland et al. 1999; Lee et al. 2012; Moran et al. 1996; Solyom et al. 2012). Within tumor types, there is wide variation of

somatic events amongst individuals, with for example a range from 0 somatic insertions to up to 79 somatic insertions per sample in squamous cell lung carcinomas.

Earlier studies found enrichment of disease-causing retrotransposon insertions on the X chromosome, possibly due to an ascertainment bias from X-linked disorders. We find cancer-associated somatic events to be evenly distributed across the autosomal and X chromosomes (Supplemental Fig. 4). The distribution of retrotransposon insertions across chromosomal arms significantly differs between germline and somatic events (Wilcoxon p=3.706e-08). Specifically, the short arm of chromosome 4 has a 1.6-fold enrichment compared to a null distribution of somatic retrotransposon insertions, differing from germline insertions in that arm (Fisher's p=0.0087).

Retrotransposons can mobilize into genic regions

Retrotransposons have the capacity to mobilize into genes and surrounding regulatory regions to affect gene expression and disrupt protein function; these insertions have previously been implicated in cancer. Most recently, Shukla et al. (2013) (Burns and Boeke 2012; Shukla et al. 2013) discovered an L1 insertion into *ST18* in hepatocellular carcinoma that resulted in overexpression of the gene. We find that the proportion of somatic retrotransposon insertions into genes is similar to that of germline events, where approximately 35% of events falling in genic regions (gene plus 1kb upstream and downstream) as would be expected from the proportion of the human genome that is comprised of these genic regions. We find several genes that are recurrently disrupted by retrotransposon insertions in multiple samples across tumor types, including *CNTNAP2*, *DLG2*, and *PDE4B* (Fig. 2A). Many of these appear to be known large, common fragile site genes (Ostertag and Kazazian 2001; Fungtammasan et al. 2012; Luan

et al. 1993; Jurka 1997; Luan and Eickbush 1995; Cost et al. 2002) (Supplemental Fig. 6A-B). A closer look at the specific genes that contain somatic insertions reveals several known cancer genes, such as *RUNX1*, a putative tumor suppressor in gastric carcinoma (Ewing and Kazazian 2011; Silva et al. 2003; Stewart et al. 2011) that is subject to recurrent loss-of-function inactivation in breast cancer and esophageal adenocarcinoma (Cordaux and Batzer 2009; Banerji et al. 2012; Dulak et al. 2012; Koboldt et al. 2012), as well as in the exon of *REV3L*, which has been implicated as a novel tumor suppressor in colorectal and lung cancers, and is involved in maintenance of genomic stability (Stewart et al. 2011; Zhang et al. 2012; Brondello et al. 2008). One UCEC sample contains an intronic somatic L1 insertion in the *ESR1* gene, an important hormone receptor often overexpressed in endometrial and breast cancers (Hancks and Kazazian 2012; Lebeau et al. 2008). While previous studies found somatic insertion only in intronic regions, we identify 21 somatic events in or within 200bp of exons of genes such as *CYR61* and *HSF2*, with seven falling in the protein coding sequence itself (Fig. 2B and Supplemental Table 3). In general, genes with somatic retrotransposon insertions tend to be involved in cell adhesion processes (Supplemental Fig. 7).

We asked whether somatic retrotransposon insertion into a gene impacts the gene's expression. Using available RNA-seq data across the eight tumor types with retrotransposon insertions in genes (LUSC, LUAD, HNSC, UCEC, BRCA, OV, COAD, and READ), we find that genes with retrotransposon insertions tend to be expressed at a lower level than the same genes in samples of the same tumor type without an insertion (KS-test p=0.006, Fig. 2C). When examined individually, genes with retrotransposition insertions show extreme expression relative to all other samples, in either direction (Fig. 2D).

Somatic 3'-sequence transductions elucidate active retrotransposition elements in cancer

In several samples, we find evidence for the retrotransposition of an L1 along with a short unique genomic sequence. These unique sequences originate from the region downstream of both reference and non-reference germline L1 elements. Known as 3'-transduction, this process is thought to result from the read-through of the weak L1 poly(A) signal and is estimated to occur in 15-23% of all genomic L1s (Miki et al. 1992; Goodier et al. 2000; Pickeral et al. 2000; Szak et al. 2002; Moran et al. 1999; Holmes et al. 1994). L1s carrying 3' transductions have been shown to disrupt several human genes in disease including *APC* (Morse et al. 1988; Miki et al. 1992), *DMD* (Iskow et al. 2010; Holmes et al. 1994), *CYBB* (Solyom et al. 2012; Meischl et al. 2000), *RP2* (Shukla et al. 2013; Schwahn et al. 1998), and *CHM* (Meyerson et al. 2010; van den Hurk et al. 2003; Stratton et al. 2009). 3'-transductions exhibit known TPRT characteristics, including TSDs, the L1 endonuclease motif at the insertion point, and poly-adenylation of the 3'-transduced segment. One HNSC sample displayed several such 3'-transduction events from different regions of the genome, suggesting that at least three separate L1HS elements were active in the tumor sample (Supplemental Table 4). In another sample, we find a known non-reference polymorphic full-length germline L1HS element (chr6:29920436) to be highly active and result in at least four separate instances of somatic 5'-truncated L1HS insertions on chromosomes 3, 9, 11, and X (Fig. 3A and Supplemental Table 4). Thus we see evidence for two models of somatic retrotransposon activity in cancer: i. a single hyperactive source element may insert itself multiple times throughout the genome in the tumor sample, and ii. multiple elements may become active in the tumor sample (Fig. 3B).

The genomic context of somatic retrotransposition

To evaluate genomic correlates of somatic retrotransposition, cases were binned into two groups by number of somatic retrotransposon insertions: Retrotransposon-High (RTI-H) tumors have greater than 10 somatic insertions and Retrotransposon-Low (RTI-L) have 10 or fewer insertions. We used the rearrangement detection tool, dRanger (Lee et al. 2012; Chapman et al. 2011; Bass et al. 2011) to identify the number of rearrangements in LUSC, LUAD and HNSC. Samples in the high somatic retrotransposition cluster have more complex genomes in terms of somatic rearrangements (Wilcoxon p=0.0097, Fig. 4A). Retrotransposon-high samples also have greater numbers of total somatic substitution mutations per sample than do retrotransposon-low samples (Wilcoxon p=2.8E-04, Fig. 4B).

Within each tumor type, we correlated somatic mutation, methylation, copy number, and miRNA data where available to retrotransposon clusters. We find that in HNSC samples, both *TP53* mutation and p16/*CDKN2A* focal deletion are significantly correlated to high retrotransposition activity (Fisher's p=0.01481, data not shown). Since HPV-positive HNSC tumors are less likely to have *TP53* mutation(Keane et al. 2013; Gillison et al. 2000; Lee et al. 2012), we looked at somatic retrotransposition versus HPV status in the 28 HNSC samples and found that, accordingly, samples with high retrotransposition are disproportionately HPV negative (Fisher's exact p=0.041, Fig. 4C).

Furthermore, we find that retrotransposons tend to insert somatically in late-replicating genes, as compared to germline insertions (Wilcoxon p=1.1E-04) and the null distribution of genic replication times (Wilcoxon p<2E-16, Fig. 4D). This is in agreement with a recent report that somatically mutated genes are biased toward later replication time (Lee et al. 2012; Lawrence et al. 2013; Beck et al. 2010; Huang et al. 2010; Hormozdiari et al. 2010; Iskow et al. 2010; Witherspoon et al. 2010; Stewart et al. 2011; Ewing and Kazazian 2010; 2011; Xing et al.

2009). Interestingly, chromatin conformation as assessed by Hi-C long-range interaction data (Lieberman-Aiden et al. 2009), shows that somatic retrotransposon insertions are targeted at regions of the genome that have a more closed conformation (Wilcoxon p=5E-04, Fig. 4E).

Finally, using RNA-seq data from LUSC tumor samples, we assessed the expression levels of two active subfamilies of retrotransposons, L1HS and *Alu*Ya5, and found that retrotransposon expression does not appear to correlate with retrotransposition activity in this tumor type (Fig. 4F).

Retrotransposon insertions identified in exome capture data

Since we find somatic retrotransposon insertions into exonic regions, we modified TranspoSeq to interrogate the large number of exome sequencing data available through TCGA. TranspoSeq-Exome locates clusters of split reads, where one portion of the read aligns uniquely to the genome and the other portion aligns to the database of consensus retrotransposon sequences, in effect, spanning the junction between unique genome and retrotransposon (Supplemental Fig. 8). This method is effective because the sequencing reads used in this study are 100bp in length and provide adequate split read sequence. We applied TranspoSeq-Exome to whole exome sequence data of 199 LUSC, 327 HNSC, and 241 UCEC samples, focusing our analysis on L1HS retotransposition. We were able to recapitulate four of the exonic insertions detected in the whole genome sequences of the same samples, and also found 22 novel somatic L1HS insertions in LUSC, 5 in UCEC and 8 in HNSC (Fig. 5A and Supplemental Table 5). Exome data reveals somatic retrotransposon insertions in exons of several of the same genes that have intronic somatic insertions in the whole genome sequencing data, as well as new exonic

insertions. Thus, we add 35 novel somatic retrotransposon events and show that somatic retrotransposon insertions into exons can be detected from hybrid-capture exome sequencing.

Notably, we find an 112bp 5'-truncated L1HS element in exon 6 of the *PTEN* tumor suppressor in DNA from an endometrial carcinoma (Fig. 5B). RNA-seq reads spanning the insertion at both ends confirm the expression of a chimeric mRNA containing a somatically inserted L1HS sequence. While its 3' end inserted at the canonical L1-endonuclease cleavage motif, this retrotransposition is likely the result of a 5' microhomology-mediated end-joining (Zingler 2005), with a 12bp overlap between reference sequence at the 5'-end integration site and the 5'-truncated L1HS element. We experimentally validated the presence and sequence of this insertion in the endometrial sample and not matched normal tissue (Supplemental Fig 9).

Discussion:

We present here a large-scale comprehensive analysis of somatic retrotransposon movement in cancer. We find that not only colorectal cancer (Lee et al. 2012; Iskow et al. 2010; Solyom et al. 2012), but also lung squamous cell, head and neck squamous cell and endometrial carcinomas exhibit considerable L1 retrotransposition. Other cancer types, including glioblastoma multiforme, acute myeloid leukemia and kidney clear cell carcinoma, remain quiet. We demonstrate the novel insertion of L1HS into known and putative tumor suppressor genes, such as *RUNX1* and *REV3L*, and identify genes that undergo recurrent insertion across samples and tumor types, such as *CNTNAP2*. We also present the first analysis of retrotransposon insertions using exome-capture data, revealing several interesting exonic insertions, including one into *PTEN*. Our findings suggest that somatic retrotransposon insertions are an important

class of cancer-associated structural variation with the potential to play a role in the tumorigenesis of certain cancers.

A small set of active L1s accounts for most of the L1 activity in humans (Brouha et al. 2002; Beck et al. 2010). We find that the majority of somatically inserted L1s are severely 5'-truncated, and are thus rendered inactive upon insertion. Nonetheless, we do identify several full-length L1HS somatic insertions, as well as common full-length germline polymorphisms that mobilize in the tumor sample, as evidenced by their transduction of unique 3'-sequences. This raises the possibility that polymorphic transposable elements in the germline may predispose to increased somatic retotransposon activity.

The typical mechanism of retrotransposition, TPRT, leads to double-stranded breaks (DSBs), and so it is thought that L1 transposition has genome-destabilizing effects (Belgnaoui et al. 2006). Whether it is the L1 that is causing these DSBs or rather contributing to L1-mediated repair of preexisting DSBs (Morrish et al. 2002) is an open question; we do, however, see some evidence of somatic L1-endonuclease-independent insertions lacking the canonical endonuclease motif and TPRT TSDs (Supplemental Fig. 5), suggesting a possible alternate mechanism of L1 insertion in tumor genomes.

The distribution of retrotransposon insertions may depend on the accessibility of the chromosome to the transposition machinery. L1-endonuclease, however, shows preference for supercoiled DNA (Feng et al. 1996), and although L1-endonuclease nicking of histone-bound DNA was found to be repressed, some sites were enhanced for L1 nicking when nucleosomal (Cost et al. 2001). We find a disproportionate amount of somatic retrotransposon insertions occurring in closed chromatin regions of the genome. Although we used chromatin open/closed states derived from a normal human lymphoblastoid cell line, Lieberman-Aiden et al. (2009)

(Lieberman-Aiden et al. 2009) found high reproducibility between cell lines of different origin and tissue type. Because genes within closed chromatin states are expressed at lower rates, it is conceivable that somatic insertions are tolerated in these regions, despite the difficulty in access.

Some limitations of TranspoSeq and TranspoSeq-Exome for identifying novel non-reference somatic retrotransposon insertions include inherent problems associated with read lengths of 100bp, fragment length dispersion, alignment uncertainty and disparate sequencing coverage. Additionally, the accuracy of retrotransposon subfamily calling is limited by the corresponding fragment length of the sequencing library. Future integration of sequencing technologies that enable long fragments and longer reads (Carneiro et al. 2012) will aid in the precise identification of the inserted elements.

In addition to identifying novel somatic retrotransposon insertions across multiple tumor and sequencing data types, we also sought to answer the question: what does somatic retrotransposition target? We show here that somatic retrotransposition recurrently targets large, common-fragile site genes that are late-replicating and tend to be located in regions of closed chromatin. Whether these regions are specifically targeted by L1 or whether negative selection eliminated the cells with insertions into other areas remains to be elucidated. L1 insertions are frequent genomic passenger events in cancer, and their ability to act as drivers has yet to be demonstrated (Rodić and Burns 2013). Thus, somatic retrotransposition should continue to be investigated in large sequencing studies such as TCGA and may provide insight into tumor biology, clinically viable targets, and potential biomarkers for patient stratification.

Methods:

Data

Sequencing data:

Sequencing data were downloaded from the TCGA CGHub repository (https://cghub.ucsc.edu/). Primary and processed data for TCGA can be downloaded by registered users at https://tcga-data.nci.nih.gov/tcga/tcgaDownload.jsp, https://cghub.ucsc.edu/. The downloaded BAM file for each tumor and normal sample (aligned to genome build hg18 for LAML, COAD, READ and two OV samples, and hg19 for all others using BWA) were used as input to TranspoSeq.

Processed RNA-seq data, in the form of RNA-seq by Expectation Maximization (RSEM) values, and mutation data were downloaded from Synapse (syn300013, https://www.synapse.org/#!Synapse:syn300013).

Retrotransposon data:

Consensus retrotransposon sequences were downloaded from GIRI RepBase (http://www.girinst.org/repbase/). All elements in the L1 (n=117) and SINE1/7SL (n=55) families, as well as SVA were included in this analysis. See Supplemental Table 6 for the sequences used. Reference retrotransposon identities were downloaded from RepeatMasker on January 12, 2013 (http://www.repeatmasker.org/).

Retrotransposon Insertion Polymorphism data:

dbRIP (Wang et al. 2006) was accessed on May 22, 2012. At the time of download, it contained 2086 *Alu*, 598 L1, and 77 SVA annotated elements. We also include data from ten other previous studies reporting germline retrotransposon insertions (Iskow et al. 2010; Burns

and Boeke 2012; Lee et al. 2012; Beck et al. 2010; Huang et al. 2010; Hormozdiari et al. 2010; Xing et al. 2009; Witherspoon et al. 2010; Stewart et al. 2011; Ewing and Kazazian 2010; 2011).

Gene Annotation data:

RefSeq annotation files for both hg18 and hg19 were downloaded from UCSC Genome Browser (genome.ucsc.edu/cgi-bin/hgTables?command=start) on Oct 19, 2011.

Computational Analysis

TranspoSeq was first presented in 2011 as RetroSeq (Helman and Meyerson 2011a; 2011b; http://cancergenome.nih.gov/newsevents/multimedialibrary/videos/retroseqhelman). It uses both paired and split read information to identify and characterize non-reference retrotransposon insertion events from tumor and matched normal BAM files. It is functionally similar to other read-anchored and split-read mobile element insertion tools such as Tea (Lee et al. 2012) and the Sanger Institute's RetroSeq (Keane et al. 2013), but includes additional *de-novo* assembly and contig alignment procedures. TranspoSeq consists of three main steps: 1) Get Reads, 2) Process Reads, and 3) Assemble Reads. See Supplemental Fig. 1 for a detailed schematic of the process.

1. Get Reads:

Beginning with the input BAM file, TranspoSeq parses out all discordant read-pairs, defined as pair-mates whose aligned positions are non-concordant with the fragment length distribution. We use a threshold of 1kb to call a non-concordant read-pair, in order balance the desired sensitivity and specificity given an average fragment length of about 400 basepairs. These read-pairs are then aligned to a database of consensus retrotransposon sequences using NCBI's blastn algorithm. Reads that align with either a predefined minimal percent identity and

number of consecutive bases, or a predefined maximal BLAST e-value are kept for further processing. In this analysis, we use a BLAST e-value threshold of 2E-07, which is equivalent to approximately 30 consecutive nucleotides with 85% identity to the consensus retrotransposon sequence. For each read that successfully aligns, we locate its pair-mate: if this mate also aligns to the retrotransposon database, the pair is discarded; if not, and the mate aligns to the genome with adequate mapping quality (MAPQ>0), the pair is collected for further processing.

2. Process Reads:

Unique reads whose pair-mates align to a retrotransposon consensus sequence are grouped by read orientation (forward or reverse) and each set is clustered separately. Clusters are defined by the distance between the start positions of two adjacent reads as no larger than 200bp. Forward and reverse clusters are then overlapped – allowing for an overlap of up to 60bp and a gap of up to 500bp between a forward and reverse cluster, in order to account for target sequence duplications (TSDs) and variable coverage. Parameter values were chosen based on prior knowledge as well as empirically, and tested on simulated datasets. One-sided events, clusters without an overlapping cluster in the opposing orientation are set aside for future investigation.

Events supported by clusters in both directions are annotated based on: presence in matched normal sample, proximity (within a 200bp window) to a reference retrotransposon, known RIP (dbRIP (Wang et al. 2006) and 1000 Genomes Project (Stewart et al. 2011; Ewing and Kazazian 2011)), known gene (RefSeq track of UCSC Genome Browser), and known CNV (Beroukhim et al. 2007). Events are also annotated with information pertaining to alignment to the retrotransposon database: identity, inferred length, and inversion status of inserted retrotransposon element.

Inferred length of an inserted element is determined computationally via the alignment positions at either end of the insertion, i.e., if the 5' junction read aligns to position 1000 of a consensus L1HS element and the 3' junction read aligns to position 6020, an inserted element of 4020bp is postulated at that site.

3. Assemble Reads:

Read-pairs supporting a candidate insertion as well as split reads spanning the putative insertion breakpoint are then assembled *de novo* using Inchworm (Grabherr et al. 2011) to form contigs in the forward and reverse directions separately. Contigs in each direction are aligned back to the database of retrotransposon consensus sequences with BLAST (blastn) and to the reference genome using BLAT. The longest contig containing a retrotransposon-aligned region and a reference-aligned region with minimal overlap is returned along with the specific retrotransposon subfamily and alignment properties. If such a contig cannot be constructed, TranspoSeq uses the alignment properties of the discordant reads themselves. Split reads are used, when available, to determine the forward and reverse breakpoints as well as the putative TSD sequence defined as the region between these forward and reverse breakpoints.

Filtering

Post-processing filtering was performed to remove regions with greater than 30% poor quality reads (MAPQ=0), less than 0.005 allelic fraction, and greater than 25 discordant reads within the candidate region in the normal sample, as well as regions that did not produce at least one substantial contig (>14bp) from *de-novo* assembly. Allelic fraction is calculated by (number of split reads supporting insertion)/(number of total reads spanning breakpoint). Candidate insertions of a retrotransposon into the same reference element subfamily were also filtered out. Only events with at least 10 read-pairs, including at least two in each direction, supporting the

insertion were maintained. Events consistent with microsatellite instability or ancient retrotransposons were filtered out. Finally, we manually reviewed each putative somatic insertion region using the Broad Institute's Integrative Genome Viewer (Robinson et al. 2011) and only those events that passed manual inspection were retained for further analysis.

TranspoSeq uses the SAMtools netsf java toolkit to parse BAM files and R for data processing. Pipelines are run with the reference assembly corresponding to the input BAMs, and the resulting calls are then converted to hg19 when necessary using UCSC Genome Browser Database liftOver (Meyer et al. 2012).

TranspoSeq-Exome

We modified TranspoSeq to search for novel junctions between retrotransposons and unique genomic sequence using split reads. Instead of aligning all discordant read-pairs to the database of consensus retrotransposon sequences, TranspoSeq-Exome first parses out all clipped reads identified by BWA and aligns the clipped sequence to the database of retrotransposons. Split reads that have >10bp aligning to a retrotransposon with an E-value of 2E-07 or lower are then clustered, processed, and annotated as in TranspoSeq (see Supplemental Fig. 8 for a schematic of the method). A limitation of this technique is that we are only able to identify inserted L1s where the 5' end (even if truncated) of the L1HS is captured, because the poly(A)-containing 3' end does not align significantly to the database. Additionally, the exact base-pair location of a clip can be misidentified by BWA.

Experimental Validation

Validations were carried out via site-specific PCR designed to span the 5' and 3' junctions of candidate insertions for tumor and matched normal samples. Primers, designed using Primer3 (Rozen and Skaletsky 2000), and target information is listed in Supplemental Table 1. PCRs were performed with 3ul of 2.5ng/ul DNA, 5 ul of 1uM mixed primers, 0.08 ul of 100mM dNTPs, 0.04 ul Hotstart Taq, 0.4 ul of 25mM MgCL2 and 1ul of 10X buffer, with 1.47 ul of dH20 for a total reaction volume of 11 ul. The reactions were run with a hot start of 95°C for 5m, then 30 cycles of 94° for 30s, 60° for 30s and 72° for 1m, followed by a final cool-down at 72° for 3min. 2ul of each PCR reaction was run on a caliper to visualize PCR amplicons. Initial PCRs underwent 8 cycles of a tailing reaction to add adapters and indexes for sequencing and run on Illumina MiSeq with single 8 bp index and standard Illumina sequencing primers, resulting in 250bp paired-end reads and insert size approximately 320bp and a coverage of ~200X. See Supplemental Fig. 9 and accompanying text for further information regarding validation experiments.

Statistical analysis

Correlations with other genomic features

Data for replication timing and chromatin conformation were collected from Chen et al. (2010) (Chen et al. 2010) and Lieberman-Aiden et al. (2009) (Lieberman-Aiden et al. 2009), respectively, and relationships with retrotransposon insertions were assessed using a two-sided Wilcoxon rank-sum test. HPV status for 28 HNSC samples were derived from the paper freeze analysis set provided by the TCGA HNSC AWG (http://www.broadinstitute.org/collaboration/gcc/samples/hnsc). These calls were based on review of several data types including detection of HPV by RNA and DNA sequencing, mass

spectrometry and available clinical data. Association between HPV status and retrotransposon insertions was quantified with a two-sided Fisher's exact test.

Retrotransposon-high and low clusters were correlated to somatic mutation, arm-level and focal copy number changes, miRNA levels and methylation data when available, using The Broad Institute's TCGA GDAC (https://confluence.broadinstitute.org/display/GDAC/Home). Fisher's exact tests are used to assess significance of association.

Sequence motif

Sequence motifs at insertion breakpoints were computed using the MEME Suite (Bailey et al. 2009).

Retrotransposon element expression

Raw RNA-seq FASTQ files were aligned to consensus L1HS and *Alu*Ya5 sequences using Bowtie 2 (Langmead et al. 2009) allowing for 1 mismatch. Values were then converted to Reads Per Kilobase per Million (RPKM) by the formula: number of mapped reads / length of transcript in kb / total number of reads in Mb.

3'-transductions

Short transductions were identified when reads on one side spanned the transduction and therefore the event maintained evidence for a retrotransposon insertion on both sides. A transduction was called when the 3' end junction of the insertion spanned across the poly(A) sequence into a region 3' of an active (either reference or germline/somatic) L1 element. Element characteristics were assessed using L1Base (Penzkofer 2004).

Correlation with gene expression

To assess overall gene expression changes across all tumor types: we compared gene expression in the sample in which the insertion is present to the distribution of RSEM across all

other samples investigated. We used a two-tailed Wilcoxon-Mann Whitney test in R to test for the hypothesis that a gene with a retrotransposon insertion is transcribed at a significantly lower level in samples with this insertion.

To assess individual expression changes: for each gene containing a retrotransposon insertion, we compared the RSEM for the sample in which the insertion is present to the empirical cumulative distribution of the RSEM values of that gene across all samples within that tumor type. We used a one-sample, two-sided Kolmogorov-Smirnov test in R (ks.test) to assess the hypothesis that a gene with a retrotransposon insertion is expressed at a significantly different level than in samples without this insertion. P-values were corrected for multiple testing using Bonferroni correction.

Data access:

Source code for TranspoSeq and TranspoSeq-Exome is available at www.broadinstitute.org/cancer/cga/transposeq. Retrotransposon insertion positions are available under the dbVar accession nstd94, at http://www.ncbi.nlm.nih.gov/dbvar/studies/nstd94/ .

Acknowledgments:

This work was conducted as part of The Cancer Genome Atlas (TCGA), a project of the National Cancer Institute (NCI) and National Human Genome Research Institute (NHGRI). We would like to thank Peter Hammerman, Chandra Pedamallu, Josh Francis, Fujiko Duke, Luc de Waal, Joonil Jung, Angela Brooks, and Alal Eran for their tremendous help. **Funding**: Funding: supported by National Cancer Institute grants U24CA143867 and U24CA126546 to M.M.

Disclosure declaration:

The authors declare no conflict of interest.

Figure Legends

Figure 1. Landscape of retrotransposon insertions across cancer reveals tumor-type specific pattern. *(A)* Distribution of duplication or deletion lengths at sites of somatic retrotransposon insertion. Target Site Duplication (TSD) lengths are sequence duplications of positive length, while microdeletions at the breakpoint are plotted as negative values according to the length of the deletion. See Supplemental Fig. 3A for an analogous plot of germline retrotransposon insertions. *(B)* A sequence logo of the consensus motif at the predicted breakpoints of somatic retrotransposon insertions. See Supplemental Fig. 3B for germline insertion sequence motif. *(C)* Total number of each retrotransposon family inserted in both tumor and matched normal (germline) and only in tumor (somatic) across all samples. *(D)* Length of somatically inserted L1 element (see Supplemental Fig. 3C for germline). *(E)* Distribution of somatic retrotransposon insertion events per individual across all tumor types. For each tumor type, the vertical axis displays the number of somatic retrotransposon events identified within each individual queried. These data are whole-genome sequences from 200 individuals collected and sequenced through The Cancer Genome Atlas, across 11 tumor types: lung adenocarcinoma (LUAD), lung squamous cell carcinoma (LUSC), ovarian carcinoma (OV), rectal adenocarcinoma (READ), colon adenocarcinoma (COAD), kidney clear cell carcinoma (KIRC), uterine corpus endometrioid carcinoma (UCEC), head and neck squamous cell carcinoma (HNSC), breast carcinoma (BRCA), acute myeloid leukemia (LAML), and glioblastoma multiforme (GBM). See Supplemental Fig. 4A-B for other representations of these data.

Figure 2. Retrotransposons can mobilize into genic regions. *(A)* Genes that contain somatic retrotransposon insertions in more than one sample. *(B)* Empirical cumulative distribution

function (ecdf) of gene expression, quantified by RNA-seq by Expectation Maximization (RSEM) values, of genes that contain somatic retrotransposon insertions in a specific sample (red) versus the ecdf of gene expression in genes that do not contain retrotransposon insertions across all other samples (black). *(C)* Genes that contain somatic retrotransposon insertions in or within 200bp of exons, 5', and 3' UTRs. *(D)* Gene expression of a selection of genes with somatic retrotransposon insertions; the red dot shows the RSEM value in the particular tumor sample that contained the retrotransposon insertion in that gene, while the grey represents the gene's expression across all other samples within that tumor type that do not contain a retrotransposon insertion.

Figure 3. 3'-transductions elucidate source retrotransposon element. *(A)* Select 3'-transduction events, including the sample, the source element location (i.e., genomic origin of the unique sequence), the transposition insertion location, and the length of the transduced sequence. See Supplemental Table 4 for a full list. *(B)* Schematic of the two models of somatic retrotransposition detected seen in this analysis: i. one source L1HS element becoming active and inserting multiple times across the tumor sample, and ii. several source elements becoming active in the tumor sample.

Figure 4. Retrotransposon load is correlated with genomic instability, late-replication and closed chromatin. *(A)* Number of somatic rearrangements in LUSC, LUAD, and HNSC samples with high retrotransposon load (>10 somatic retrotransposon insertions, RTI-H) and with low retrotransposon load (<=10 somatic insertion, RTI-L). *(B)* Number of somatic mutations in RTI-H and RTI-L samples across all 11 tumor types. *(C)* HPV status of RTI-H and RTI-L HNSC

samples. *(D)* Replication timing of genes that contain somatic retrotransposon insertions versus genes that contain germline insertions, and all RefSeq genes. Later replicating genes have higher values of replication time on the y-axis. *(E)* Chromatin conformation of genes that contain somatic retrotransposon insertions versus genes that contain germline insertions, and all RefSeq genes. The y-scale represents relative chromatin "openness", the lower the y-value, the more closed the chromatin state. *(F)* Expression (RPKM) of consensus L1HS and *Alu*Ya5 sequences in RTI-H and RTI-L LUSC samples. All error bars represent standard error of the distribution.

Figure 5. Exome sequencing identifies novel retrotransposon insertions into exons. *(A)* Genes with somatic retrotransposon insertions into exons as detected by TranspoSeq-Exome. Somatic insertions in *PPFIA2*, *PCNX*, and *CRB1* were identified in the whole-genome sequencing cohort as well as in separate samples in the exome sequencing set. *(B)* Diagram of a 90bp 5'-truncated L1HS element inserted into exon 6 of *PTEN*. In blue are RNA-seq reads that span the reference-transposon junction, supporting its expression.

References:

Bailey TL, Boden M, Buske FA, Frith M, Grant CE, Clementi L, Ren J, Li WW, Noble WS. 2009. MEME SUITE: tools for motif discovery and searching. *Nucleic Acids Research* **37**: W202–W208.

Banerji S, Cibulskis K, Rangel-Escareno C, Brown KK, Carter SL, Frederick AM, Lawrence MS, Sivachenko AY, Sougnez C, Zou L, et al. 2012. Sequence analysis of mutations and translocations across breast cancer subtypes. *Nature* **486**: 405–409.

Bass AJ, Lawrence MS, F B, Ramos AH, Drier Y, Cibulskis K, Sougnez C, Voet D, Saksena G, Sivachenko A, et al. 2011. Genomic sequencing of colorectal adenocarcinomas identifies a recurrent VTI1A-TCF7L2 fusion. *Nat Genet* **43**: 964–968.

Beck CR, Collier P, Macfarlane C, Malig M, Kidd JM, Eichler EE, Badge RM, Moran JV. 2010. LINE-1 Retrotransposition Activity in Human Genomes. *Cell* **141**: 1159–1170.

Belgnaoui SM, Gosden RG, Semmes OJ, Haoudi A. 2006. Human LINE-1 retrotransposon induces DNA damage and apoptosis in cancer cells. *Cancer Cell Int* **6**: 13.

Beroukhim R, Getz G, Nghiemphu L, Barretina J, Hsueh T, Linhart D, Vivanco I, Lee JC, Huang JH, Alexander S, et al. 2007. Assessing the significance of chromosomal aberrations in cancer: methodology and application to glioma. *Proc Natl Acad Sci USA* **104**: 20007–20012.

Brondello J-M, Pillaire MJ, Rodriguez C, Gourraud P-A, Selves J, Cazaux C, Piette J. 2008. Novel evidences for a tumor suppressor role of Rev3, the catalytic subunit of Pol ζ. *Oncogene* **27**: 6093–6101.

Brouha B, Meischl C, Ostertag E, de Boer M, Zhang Y, Neijens H, Roos D, Kazazian HH. 2002. Evidence consistent with human L1 retrotransposition in maternal meiosis I. *Am J Hum Genet* **71**: 327–336.

Brouha B, Schustak J, Badge RM, Lutz-Prigge S, Farley AH, Moran JV, Kazazian HH. 2003. Hot L1s account for the bulk of retrotransposition in the human population. *Proc Natl Acad Sci USA* **100**: 5280–5285.

Burns KH, Boeke JD. 2012. Human Transposon Tectonics. *Cell* **149**: 740–752.

Carneiro MO, Russ C, Ross MG, Gabriel SB, Nusbaum C, DePristo MA. 2012. Pacific biosciences sequencing technology for genotyping and variation discovery in human data. *BMC Genomics* **13**: 1–1.

Chapman MA, Lawrence MS, Keats JJ, Cibulskis K, Sougnez C, Schinzel AC, Harview CL, Brunet J-P, Ahmann GJ, Adli M, et al. 2011. Initial genome sequencing and analysis of multiple myeloma. *Nature* **471**: 467–472.

Chen CL, Rappailles A, Duquenne L, Huvet M, Guilbaud G, Farinelli L, Audit B, d'Aubenton-

Carafa Y, Arneodo A, Hyrien O, et al. 2010. Impact of replication timing on non-CpG and CpG substitution rates in mammalian genomes. *Genome Research* **20**: 447–457.

Cordaux R, Batzer MA. 2009. The impact of retrotransposons on human genome evolution. *Nature Reviews Genetics* **10**: 691–703.

Cost GJ, Feng Q, Jacquier A, Boeke JD. 2002. Human L1 element target-primed reverse transcription in vitro. *EMBO J* **21**: 5899–5910.

Cost GJ, Golding A, Schlissel MS, Boeke JD. 2001. Target DNA chromatinization modulates nicking by L1 endonuclease. *Nucleic Acids Research* **29**: 573–577.

Dulak AM, Schumacher SE, van Lieshout J, Imamura Y, Fox C, Shim B, Ramos AH, Saksena G, Baca SC, Baselga J, et al. 2012. Gastrointestinal Adenocarcinomas of the Esophagus, Stomach, and Colon Exhibit Distinct Patterns of Genome Instability and Oncogenesis. *Cancer Res* **72**: 4383–4393.

Ewing AD, Kazazian HH. 2010. High-throughput sequencing reveals extensive variation in human-specific L1 content in individual human genomes. *Genome Research* **20**: 1262–1270.

Ewing AD, Kazazian HH. 2011. Whole-genome resequencing allows detection of many rare LINE-1 insertion alleles in humans. *Genome Research* **21**: 985–990.

Feng Q, Moran JV, Kazazian HH, Boeke JD. 1996. Human L1 retrotransposon encodes a conserved endonuclease required for retrotransposition. *Cell* **87**: 905–916.

Fungtammasan A, Walsh E, Chiaromonte F, Eckert KA, Makova KD. 2012. A genome-wide analysis of common fragile sites: What features determine chromosomal instability in the human genome? *Genome Research* **22**: 993–1005.

Gillison ML, Koch WM, Capone RB, Spafford M, Westra WH, Wu L, Zahurak ML, Daniel RW, Viglione M, Symer DE, et al. 2000. Evidence for a causal association between human papillomavirus and a subset of head and neck cancers. *J Natl Cancer Inst* **92**: 709–720.

Goodier JL, Ostertag EM, Kazazian HH. 2000. Transduction of 3'-flanking sequences is common in L1 retrotransposition. *Human Molecular Genetics* **9**: 653–657.

Grabherr MG, Haas BJ, Yassour M, Levin JZ, Thompson DA, Amit I, Adiconis X, Fan L, Raychowdhury R, Zeng Q, et al. 2011. Full-length transcriptome assembly from RNA-Seq data without a reference genome. *Nature Publishing Group* **29**: 644–652.

Hancks DC, Kazazian HH Jr. 2012. Active human retrotransposons: variation and disease. *Current Opinion in Genetics & Development* **22**: 191–203.

Helman E, Meyerson M. 2011a. RetroSeq: A Tool To Discover Somatic Insertion of Retrotransposons - Elena Helman - TCGA. *cancergenomenihgov*. http://cancergenome.nih.gov/newsevents/multimedialibrary/videos/retroseqhelman (Accessed June 4, 2013a).

Helman E, Meyerson M. 2011b. Translation of the Cancer Genome Program. *aacrorg*. http://www.aacr.org/home/scientists/meetings--workshops/special-conferences/previous-special-conferences/2011---2012-special-conferences/translation-of-the-cancer-genome/program.aspx (Accessed June 7, 2013b).

Holmes SE, Dombroski BA, Krebs CM, Boehm CD, Kazazian HH. 1994. A new retrotransposable human L1 element from the LRE2 locus on chromosome 1q produces a chimaeric insertion. *Nat Genet* **7**: 143–148.

Hormozdiari F, Hajirasouliha I, Dao P, Hach F, Yorukoglu D, Alkan C, Eichler EE, Sahinalp SC. 2010. Next-generation VariationHunter: combinatorial algorithms for transposon insertion discovery. *Bioinformatics* **26**: i350–i357.

Huang CRL, Schneider AM, Lu Y, Niranjan T, Shen P, Robinson MA, Steranka JP, Valle D, Civin CI, Wang T, et al. 2010. Mobile Interspersed Repeats Are Major Structural Variants in the Human Genome. *Cell* **141**: 1171–1182.

Iskow RC, McCabe MT, Mills RE, Torene S, Pittard WS, Neuwald AF, Van Meir EG, Vertino PM, Devine SE. 2010. Natural Mutagenesis of Human Genomes by Endogenous Retrotransposons. *Cell* **141**: 1253–1261.

Jurka J. 1997. Sequence patterns indicate an enzymatic involvement in integration of mammalian retroposons. *Proc Natl Acad Sci USA* **94**: 1872–1877.

Kazazian HH. 2004. Mobile Elements: Drivers of Genome Evolution. *Science* **303**: 1626–1632.

Keane TM, Wong K, Adams DJ. 2013. RetroSeq: transposable element discovery from next-generation sequencing data. *Bioinformatics* **29**: 389–390.

Kimberland ML, Divoky V, Prchal J, Schwahn U, Berger W, Kazazian HH. 1999. Full-length human L1 insertions retain the capacity for high frequency retrotransposition in cultured cells. *Human Molecular Genetics* **8**: 1557–1560.

Koboldt DC, Fulton RS, McLellan MD, Schmidt H, Kalicki-Veizer J, McMichael JF, Fulton LL, Dooling DJ, Ding L, Mardis ER, et al. 2012. Comprehensive molecular portraits of human breast tumours. *Nature* **490**: 61–70.

Lander ES, Linton LM, Birren B, Nusbaum C, Zody MC, Baldwin J, Devon K, Dewar K, Doyle M, FitzHugh W, et al. 2001. Initial sequencing and analysis of the human genome. *Nature* **409**: 860–921.

Langmead B, Trapnell C, Pop M, Salzberg SL. 2009. Ultrafast and memory-efficient alignment of short DNA sequences to the human genome. *Genome Biol* **10**: R25.

Lawrence MS, Stojanov P, Polak P, Kryukov GV, Cibulskis K, Sivachenko A, Carter SL, Stewart C, Mermel CH, Roberts SA, et al. 2013. Mutational heterogeneity in cancer and the search for new cancer-associated genes. *Nature* **499**: 214–218.

Lebeau A, Grob TJ, Holst F, Seyedi-Fazlollahi N, Moch H, Terracciano L, Turzynski A, Choschzick M, Sauter G, Simon R. 2008. Oestrogen receptor gene (ESR1) amplification is frequent in endometrial carcinoma and its precursor lesions. *J Pathol* **216**: 151–157.

Lee E, Iskow R, Yang L, Gokcumen O, Haseley P, Luquette LJ, Lohr JG, Harris CC, Ding L, Wilson RK, et al. 2012. Landscape of Somatic Retrotransposition in Human Cancers. *Science* **337**: 967–971.

Lieberman-Aiden E, van Berkum NL, Williams L, Imakaev M, Ragoczy T, Telling A, Amit I, Lajoie BR, Sabo PJ, Dorschner MO, et al. 2009. Comprehensive Mapping of Long-Range Interactions Reveals Folding Principles of the Human Genome. *Science* **326**: 289–293.

Luan DD, Eickbush TH. 1995. RNA template requirements for target DNA-primed reverse transcription by the R2 retrotransposable element. *Mol Cell Biol* **15**: 3882–3891.

Luan DD, Korman MH, Jakubczak JL, Eickbush TH. 1993. Reverse transcription of R2Bm RNA is primed by a nick at the chromosomal target site: a mechanism for non-LTR retrotransposition. *Cell* **72**: 595–605.

Meischl C, Boer M, Ahlin A, Roos D. 2000. A new exon created by intronic insertion of a rearranged LINE-1 element as the cause of chronic granulomatous disease. *Eur J Hum Genet* **8**: 697–703.

Meyer LR, Zweig AS, Hinrichs AS, Karolchik D, Kuhn RM, Wong M, Sloan CA, Rosenbloom KR, Roe G, Rhead B, et al. 2012. The UCSC Genome Browser database: extensions and updates 2013. *Nucleic Acids Research* **41**: D64–D69.

Meyerson M, Gabriel S, Getz G. 2010. Advances in understanding cancer genomes through second-generation sequencing. *Nature Reviews Genetics* **11**: 685–696.

Miki Y, Nishisho I, Horii A, Miyoshi Y, Utsunomiya J, Kinzler KW, Vogelstein B, Nakamura Y. 1992. Disruption of the APC gene by a retrotransposal insertion of L1 sequence in a colon cancer. *Cancer Res* **52**: 643–645.

Moran JV, DeBerardinis RJ, Kazazian HH. 1999. Exon shuffling by L1 retrotransposition. *Science* **283**: 1530–1534.

Moran JV, Holmes SE, Naas TP, DeBerardinis RJ, Boeke JD, Kazazian HH. 1996. High frequency retrotransposition in cultured mammalian cells. *Cell* **87**: 917–927.

Morrish TA, Gilbert N, Myers JS, Vincent BJ, Stamato TD, Taccioli GE, Batzer MA, Moran JV. 2002. DNA repair mediated by endonuclease-independent LINE-1 retrotransposition. *Nat Genet* **31**: 159–165.

Morse B, Rotherg PG, South VJ, Spandorfer JM, Astrin SM. 1988. Insertional mutagenesis of the myc locus by a LINE-1 sequence in a human breast carcinoma. *Nature* **333**: 87–90.

Ostertag EM, Kazazian HH. 2001. Biology of mammalian L1 retrotransposons. *Annu Rev Genet*

35: 501–538.

Penzkofer T. 2004. L1Base: from functional annotation to prediction of active LINE-1 elements. *Nucleic Acids Research* **33**: D498–D500.

Pickeral OK, Makałowski W, Boguski MS, Boeke JD. 2000. Frequent human genomic DNA transduction driven by LINE-1 retrotransposition. *Genome Research* **10**: 411–415.

Robinson JT, Thorvaldsdóttir H, Winckler W, Guttman M, Lander ES, Getz G, Mesirov JP. 2011. Integrative genomics viewer. *Nature Publishing Group* **29**: 24–26.

Rodić N, Burns KH. 2013. Long Interspersed Element–1 (LINE-1): Passenger or Driver in Human Neoplasms? ed. S.M. Rosenberg. *PLoS Genet* **9**: e1003402.

Rozen S, Skaletsky H. 2000. Primer3 on the WWW for general users and for biologist programmers. *Methods Mol Biol* **132**: 365–386.

Schwahn U, Lenzner S, Dong J, Feil S, Hinzmann B, van Duijnhoven G, Kirschner R, Hemberger M, Bergen AA, Rosenberg T, et al. 1998. Positional cloning of the gene for X-linked retinitis pigmentosa 2. *Nat Genet* **19**: 327–332.

Shukla R, Upton KR, Muñoz-Lopez M, Gerhardt DJ, Fisher ME, Nguyen T, Brennan PM, Baillie JK, Collino A, Ghisletti S, et al. 2013. Endogenous Retrotransposition Activates Oncogenic Pathways in Hepatocellular Carcinoma. *Cell* **153**: 101–111.

Silva FPG, Morolli B, Storlazzi CT, Anelli L, Wessels H, Bezrookove V, Kluin-Nelemans HC, Giphart-Gassler M. 2003. Identification of RUNX1/AML1 as a classical tumor suppressor gene. *Oncogene* **22**: 538–547.

Solyom S, Ewing AD, Rahrmann EP, Doucet TT, Nelson HH, Burns MB, Harris RS, Sigmon DF, Casella A, Erlanger B, et al. 2012. Extensive somatic L1 retrotransposition in colorectal tumors. *Genome Research*.

Stewart C, Kural D, Strömberg MP, Walker JA, Konkel MK, Stütz AM, Urban AE, Grubert F, Lam HYK, Lee W-P, et al. 2011. A Comprehensive Map of Mobile Element Insertion Polymorphisms in Humans ed. H.S. Malik. *PLoS Genet* **7**: e1002236.

Stratton MR, Campbell PJ, Futreal PA. 2009. The cancer genome. *Nature* **458**: 719–724.

Szak ST, Pickeral OK, Makalowski W, Boguski MS, Landsman D, Boeke JD. 2002. Molecular archeology of L1 insertions in the human genome. *Genome Biol* **3**: research0052.

van den Hurk JAJM, van de Pol DJR, Wissinger B, van Driel MA, Hoefsloot LH, de Wijs IJ, van den Born LI, Heckenlively JR, Brunner HG, Zrenner E, et al. 2003. Novel types of mutation in the choroideremia (CHM) gene: a full-length L1 insertion and an intronic mutation activating a cryptic exon. *Hum Genet* **113**: 268–275.

Wang J, Song L, Grover D, Azrak S, Batzer MA, Liang P. 2006. dbRIP: a highly integrated

database of retrotransposon insertion polymorphisms in humans. *Hum Mutat* **27**: 323–329.

Witherspoon DJ, Xing J, Zhang Y, Watkins WS, Batzer MA, Jorde LB. 2010. Mobile element scanning (ME-Scan) by targeted high-throughput sequencing. *BMC Genomics* **11**: 410.

Xing J, Zhang Y, Han K, Salem AH, Sen SK, Huff CD, Zhou Q, Kirkness EF, Levy S, Batzer MA, et al. 2009. Mobile elements create structural variation: Analysis of a complete human genome. *Genome Research* **19**: 1516–1526.

Zhang S, Chen H, Zhao X, Cao J, Tong J, Lu J, Wu W, Shen H, Wei Q, Lu D. 2012. REV3L 3′UTR 460 T>C polymorphism in microRNA target sites contributes to lung cancer susceptibility. 1–9.

Zingler N. 2005. Analysis of 5“ junctions of human LINE-1 and Alu retrotransposons suggests an alternative model for 5-”end attachment requiring microhomology-mediated end-joining. *Genome Research* **15**: 780–789.

Figure 1

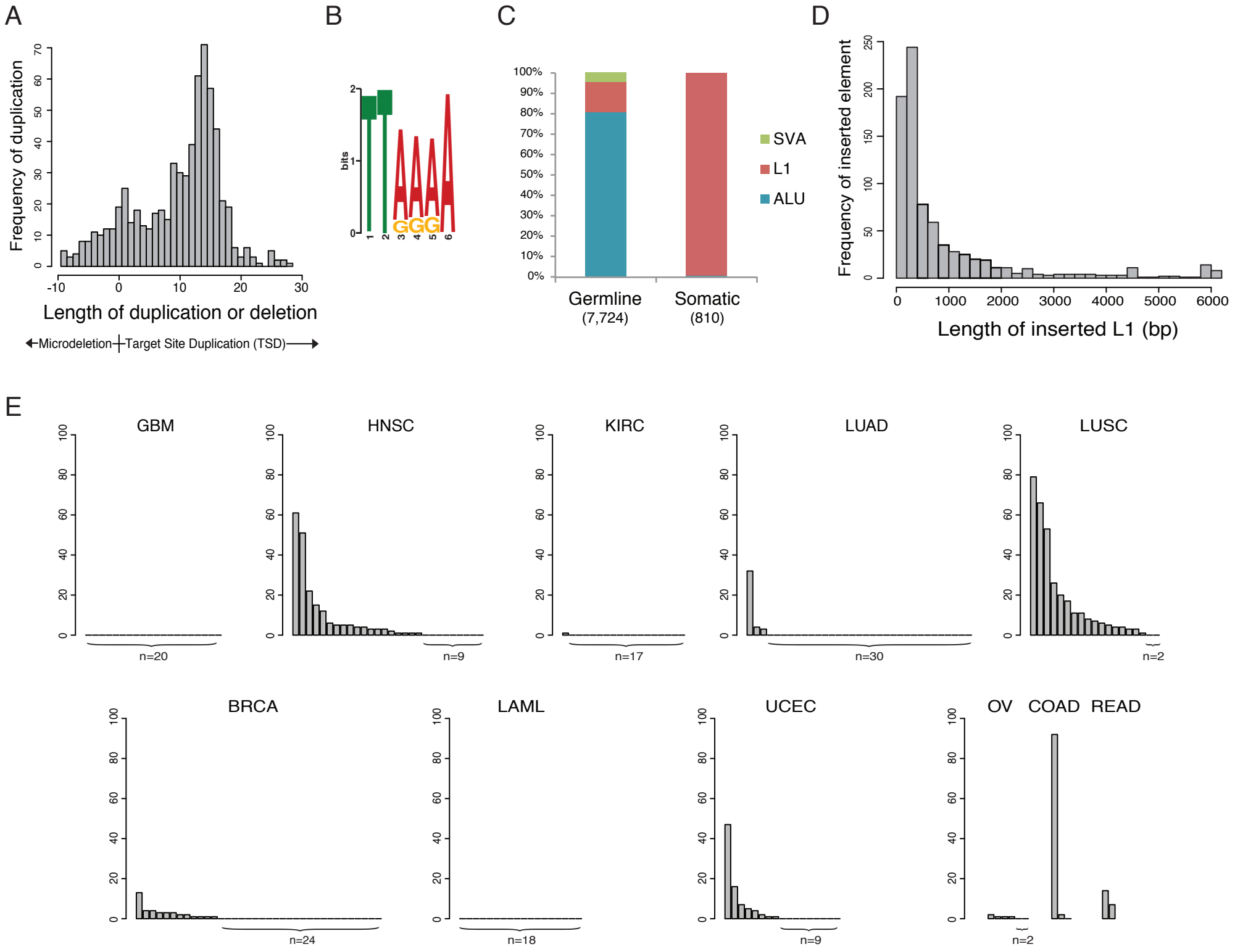
A
Frequency of duplication
Length of duplication or deletion
Microdeletion
Target Site Duplication (TSD)
B
bits
C
SVA
L1
ALU
Germline
(7,724)
Somatic
(810)
D
Frequency of inserted element
Length of inserted L1 (bp)
E
GBM
HNSC
KIRC
LUAD
LUSC
BRCA
LAML
UCEC
OV
COAD
READ
n=20
n=9
n=17
n=30
n=2
n=24
n=18
n=9
n=2

Figure 2

A

Gene	Samples with somatic insertion
CNTNAP2	LUSC-43-3920; LUSC-60-2711; LUSC-66-2766; UCEC-A5-A0GA
CTNNA2	LUSC-21-1076; HNSC-BA-4076; COAD-AA-3518
MDGA2	LUSC-60-2711; LUSC-66-2766; HNSC-BA-4076
AGMO	LUSC-43-3394; LUSC-60-2711
ARHGAP15	LUSC-60-2698; HNSC-CR-6487
BBS9	LUSC-60-2713; UCEC-A5-A0GA
CSMD1	HNSC-CV-7180 (2)
DLG2	LUSC-60-2713; HNSC-BA-4076
EYS	LUSC-60-2698; COAD-AA-3518
FAM19A2	LUSC-43-3920; UCEC-A5-A0GA
LRRTM4	UCEC-A5-A0GA; HNSC-CR-6472
MAGI2	LUSC-60-2724; HNSC-CV-5442
PDE4B	LUSC-60-2711; UCEC-AP-A052
RIMS1	HNSC-CN-5374; COAD-AA-3518
SEMA3E	LUSC-60-2711; LUSC-66-2766
DAB1	LUSC-34-2600; LUAD-38-4630
GRID2	HNSC-CV-7255; OV-25-1319

B

Sample	Gene	Region
LUAD-38-4630	*CYR61*	Exon 4
LUSC-43-3920	*REV3L*	Exon 12
LUSC-60-2726	*ZNF267*	Exon 4
LUSC-66-2766	*HSF2*	Exon 10
LUSC-66-2766	*PBLD*	Exon 3
HNSC-CR-6470	*ANKRD18A*	Exon 15
HNSC-CV-6433	*GUCY1B2*	Exon 4
COAD-AA-3518	*GPATCH2*	3' UTR
LUSC-60-2698	*C20orf107*	3' UTR
HNSC-CV-5442	*TRDMT1*	3' UTR
LUSC-60-2698	*DHRS7B*	13bp before exon3
HNSC-BA-6873	*TNIP3*	22bp before 5'UTR
LUSC-66-2766	*C3orf33*	59bp before exon4
HNSC-BA-6873	*ERO1L*	94bp after exon10

C

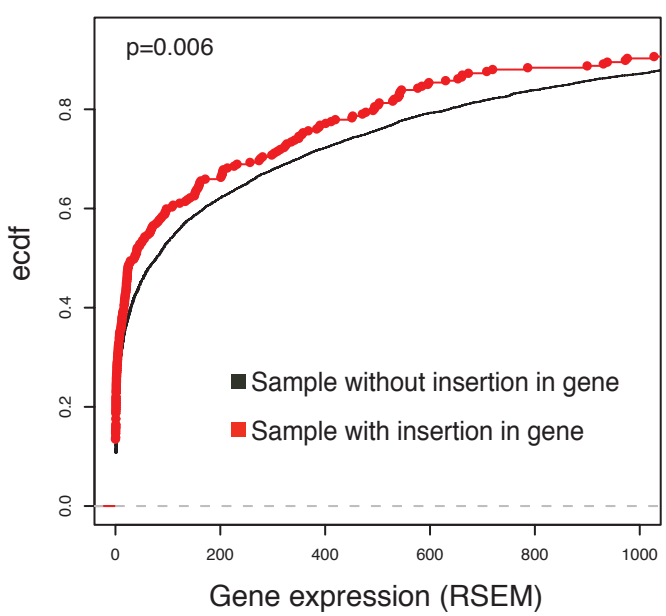

D

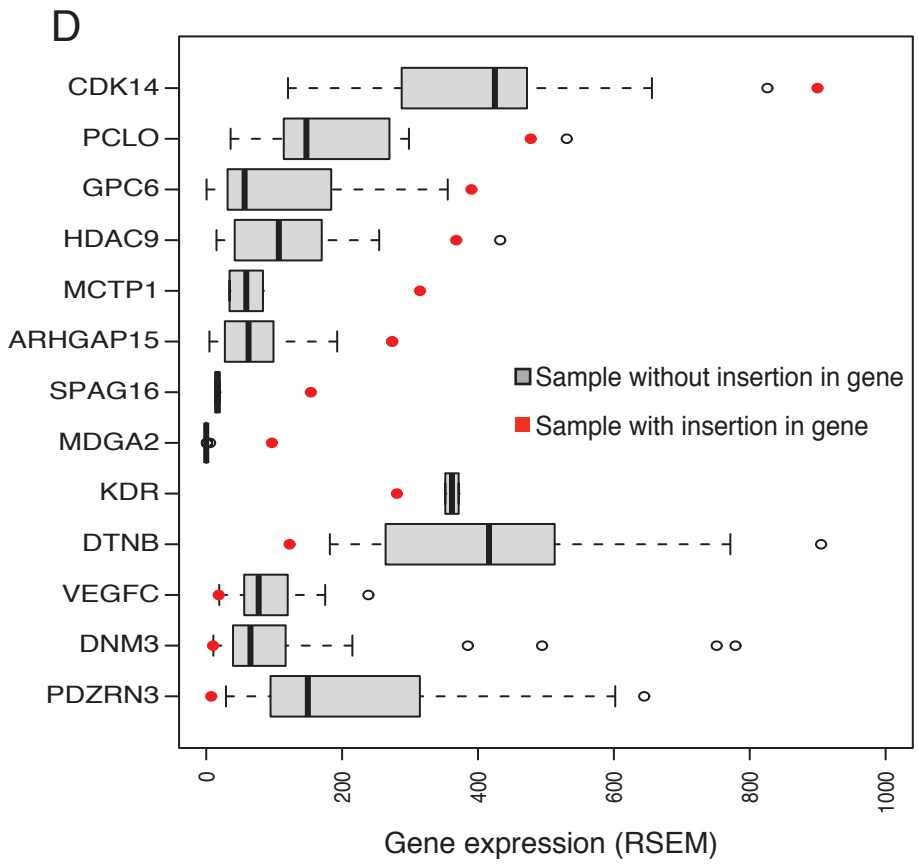

Figure 3

A

Sample	Source element	Somatic insertions	Length of 3' Transduction
TCGA-BA-4076	Full-length Ta1-nd germline L1HS at chr8:57161596	Chr10	480bp
TCGA-BA-4076	Full-length Ta1-nd reference L1HS at chr22:29059272	Chr2, ChrX, Chr8	604bp
TCGA-BA-4076	Full-length Ta1-d reference L1HS at chr8:135082972	Chr4	528bp
TCGA-BA-5873	Full-length Ta1-nd germline L1HS at chr3:55788568	Chr4	523bp
TCGA-CV-7180	Full-length Ta1-d germline L1HS at chr6:29920436	Chr3, Chr9, Chr11, ChrX	412bp

B

i. one source element, multiple insertions

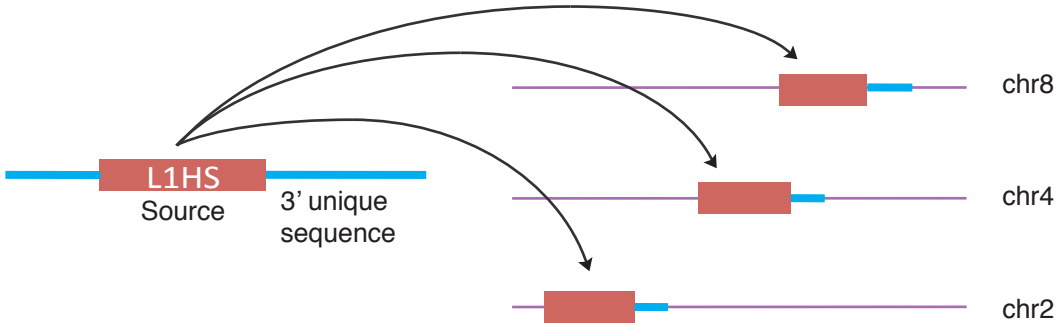

ii. multiple source elements

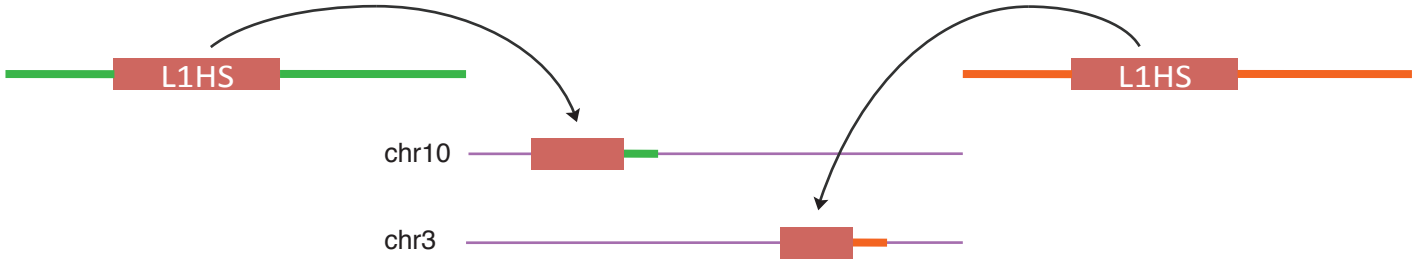

Figure 4

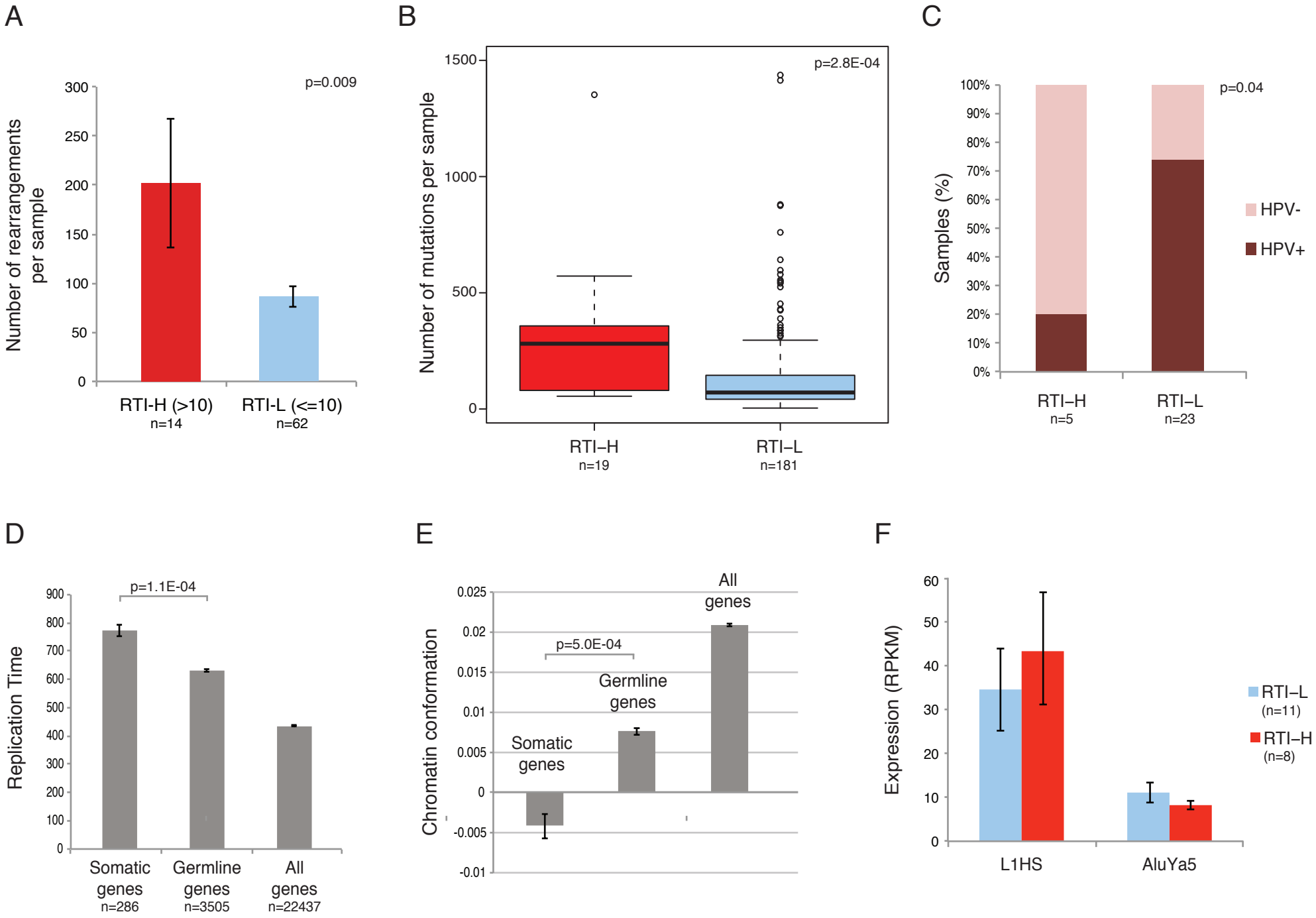
A
p=0.009
Number of rearrangements per sample
300
250
200
150
100
50
0
RTI-H (>10)
n=14
RTI-L (<=10)
n=62
B
p=2.8E-04
Number of mutations per sample
1500
1000
500
0
RTI–H
n=19
RTI–L
n=181
C
p=0.04
Samples (%)
100%
90%
80%
70%
60%
50%
40%
30%
20%
10%
0%
HPV-
HPV+
RTI–H
n=5
RTI–L
n=23
D
p=1.1E-04
Replication Time
900
800
700
600
500
400
300
200
100
0
Somatic genes
n=286
Germline genes
n=3505
All genes
n=22437
E
Chromatin conformation
0.025
0.02
0.015
0.01
0.005
0
-0.005
-0.01
p=5.0E-04
All genes
Germline genes
Somatic genes
F
Expression (RPKM)
60
50
40
30
20
10
0
RTI–L
(n=11)
RTI–H
(n=8)
L1HS
AluYa5

Figure 5

A

Gene	Sample	Region
PPFIA2	LUSC-60-2711(WGS); UCEC-AP-A0LF (Capture)	14kb after exon29 (WGS); 121bp before exon5 (Capture)
PCNX	LUSC-66-2766(WGS); LUSC-66-2758 (Capture)	1kb after exon29 (WGS); 48bp before exon14 (Capture)
CRB1	LUSC-60-2698(WGS); LUSC-22-4593 (Capture)	9kb after exon9 (WGS); Exon 7 (Capture)
PTEN	UCEC-BG-A0VV	Exon 6
FAP	UCEC-BG-A0M9	22bp before exon9
CP10	LUSC-43-2578	Exon 11
CABLES1	LUSC-60-2698	87bp after exon2
BCHE	LUSC-60-2708	71bp after exon1
DPF3	LUSC-66-2777	87bp after exon1
PLD1	HNSC-CQ-5332	80bp before exon7
APOL2	HNSC-DQ-5629	3bp after exon1

B